ISSN 1392–1320 MATERIALS SCIENCE (MEDŽIAGOTYRA). Vol. 11, No. 3. 2005

Image-Analysis-Based Measuring of Lateral Deformation of Hardening Concrete

Petr ŠTEMBERK*, Alena KOHOUTKOVÁ

Deptartment of Concrete Structures and Bridges, Faculty of Civil Engineering, Czech Technical University, Thákurova 7, 166 29 Prague 6, Czech Republic

Received 21 February 2005; accepted 12 May 2005

At present, there is no special testing method for measuring the lateral deformation of solidifying and hardening concrete. Contact methods, which are used for already hardened concrete, are not suitable due to either their incapability of attaching the measuring equipment to the surface of a specimen or the lack of adhesion in case of application of embedded strain gauges. The use of laser sensors also is not suitable for application since the longitudinal deformation of hardening concrete is quite large, which requires some mobile attachment of the laser sensor so that it can follow the targeted spot with progressing longitudinal deformation. An optical method where an image is captured with a high-resolution CCD camera is relatively easy and nowadays also inexpensive. Capturing an image solves the part of acquiring test data on the lateral deformation, however, conversion of image data to lateral deformation measurement requires an adequate method, which is described in this paper.
Keywords: hardening concrete, image analysis, Poisson's ratio.

1. INTRODUCTION

The growing demand for accelerated execution of concrete structures requires some extra knowledge about the material parameters of concrete at extremely early ages, which means the age of up to one day. During the first half of this period, concrete undergoes a transition from a liquid to a solid state. Methods for investigation of material characteristics of fresh concrete are known and they are also mostly standardized, same as the methods for evaluation of mechanical properties of already hardened concrete. However, the transient state of concrete brings about numerous difficulties related to the rapidly changing consistency of concrete, which means that the testing methods designed for either fresh or already hardened concrete cannot by applied.

Simple techniques based on the uniaxial compression and penetration tests were proposed and the experiments yielded, from today's point of view, very useful data on the evolution of modulus of elasticity and compressive strength of solidifying and further hardening concrete, e.g. [1, 2]. Implementation of new accelerated technologies of execution, however, requires a rigorous multi-dimensional analysis of mechanical behavior of concrete subjected to excessive loading at such early ages and, therefore, it is necessary to provide a realistic value of Poisson's ratio. It can be found in a non-technical paper, [3], that the Poisson's ratio of fresh concrete may be as high as 0.42 and also, a promising function describing the evolution of the Poisson's ratio is proposed. Because no exact range of application of this function is given, it can be used only as a hint. Of course, it is presumable that the evolution of the Poisson's ratio depends on the progressing hydration, nevertheless an affordable means of its quantification should be available.

While the measurement of longitudinal deformation of a test specimen is relatively easy, the measurement of lateral deformation of solidifying and hardening concrete requires special treatment for two reasons. Firstly, the surface of a stripped specimen is relatively soft which prohibits any attachment of strain gauges to the specimen and, secondly, the longitudinal deformation of yet hardening concrete is large, therefore, in order to measure the lateral deformation at the same spot, the measuring equipment has to follow the measured spot with progressing longitudinal deformation. For those two reasons one needs to be careful while opting for a measuring method. A method based on capturing images by a high-resolution CCD camera with subsequent image processing represents an affordable method with reasonable accuracy.

In this paper, a method of measuring the lateral deformation of yet hardening concrete is described and some representative results obtained from experiments are shown. The method consists of capturing images during the standard uniaxial compression test and the acquisition of lateral deformation measurements from the captured images by image processing, which is described in detail. This method can be used at the ages after the initial setting time when it is possible to demold a concrete specimen.

2. LATERAL DEFORMATION MEASUREMENT

2.1. Available Techniques

Basically, the methods for measuring the lateral deformation of solidifying and hardening concrete can be divided into two groups, the contact methods and the contact-free methods. The main difference between these two groups is that contact methods impose certain stress at the contact points, which may not be negligible, whereas contact-free methods avoid this drawback. On the other hand, the contact-free methods in comparison with the contact methods can be rather costly. If one considers a contact method, the constraining effect of the measuring device needs to be taken into account. This is due to the

*Corresponding author. Tel.: +420-224-354364; fax.: +420-233-335797.
E-mail address: *stemberk@fsv.cvut.cz* (P. Štemberk)

soft consistency of the hardening concrete which prohibits any use of devices whose cross-sectional area at the point of contact is small. The needle-like sensors, which are commonly used for already hardened concrete, would penetrate the soft surface of a specimen and thus reduce the quality of measured data. Also, such devices are usually attached to the testing machine without any requirement on the measuring device to follow the originally measured spot since the longitudinal deformation of already hardened concrete is negligible in comparison with that of solidifying or hardening concrete. A possible solution for avoiding the penetration of the measuring device into the specimen surface and concurrently to allow the measuring device to maintain the original location of measurement is to introduce a ring which is set around the specimen and which follows the circumferential deformation (Fig. 1). This solution contains a drawback related to the friction between the ring and the specimen surface. In the case of hardened concrete this effect is overcome by using a ring made of small cylinders which are connected into a chain. In the case of hardening concrete, such a simple solution does not exist as the soft surface of the specimen prohibits its use.

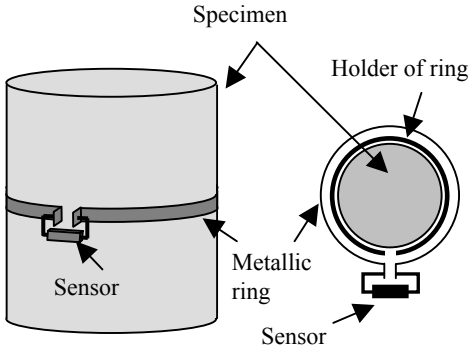

Fig. 1. Contact method configuration

Regarding the contact-free methods, the most common methods for measuring lateral deformation use the laser sensor. Depending on surface conditions and quality of the laser sensor, laser sensors sometimes require pasting a marker on the measured spot, which does not constitute a significant drawback, nevertheless, technically it is rather difficult to paste a marker to a wet surface of a less cohesive material. In the case of solidifying and hardening concrete, however, the measured spot shifts with progressing longitudinal deformation which needs to be reflected by using a mobile attachment. Such equipment is not always at hand and it may represent an unnecessary source of errors. A contact-free method which is based on image capturing and processing, in this light, seems to be more reasonable since the number of measured points and its overall accuracy are limited only by the resolution of a digital camera, or a scanner, which, at present, is already very high and therefore does not represent any constraint.

2.2. Optical Approach

An optical method where an image is captured with a high resolution CCD camera is relatively easy and nowadays also inexpensive. For that reason it was decided to develop an optical method for measuring lateral deformation of solidifying and hardening concrete. Compared with the drawbacks of the above mentioned methods, there is no friction between a camera and a specimen, and capturing of an image solves the part of measuring at the same spot, or spots, because once the targeted spot is marked, it is easy to be identified in the captured image.

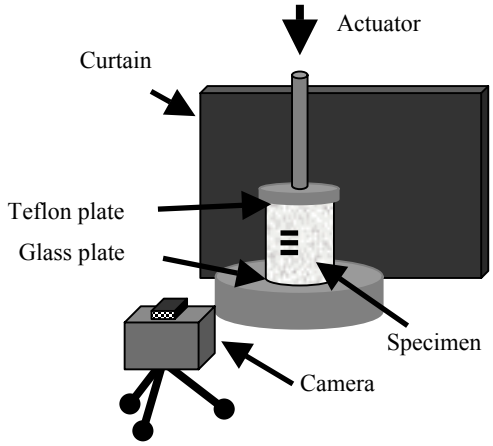

Fig. 2. Optical-based test configuration

In this case, a CCD camera with resolution of 3040×2016 pixels was used. In order to pronounce the edge of a specimen, a dark curtain was installed behind the test set and a specimen was illuminated on both sides with two spotlights, as shown in Fig. 2. The focus of the camera was set in advance and kept constant. The shutter of the camera was correlated in terms of time with a PC collected data on longitudinal displacement measured by LVDT (stroke 200 mm) and loading force measured by a load cell. An example of a captured image is shown in Fig. 3.

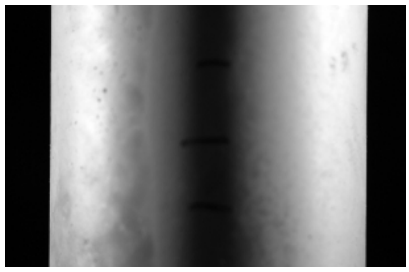

Fig. 3. Captured image of specimen

3. IMAGE PROCESSING

Three strips were cut from the captured image. The monochromatic bitmap image comprising data in the form of 256 grades of gray scale was converted to an array of digits for each pixel. In order to detect the edges of a specimen on the subpixel domain, the center of gravity of the area under the curve defined by the grade differences of neighboring pixels, shown in Fig. 4, is calculated. The distance between the centers of gravity on both sides of a specimen defines the width of the specimen. However, because the distance of the camera from a specimen is of about the same order as the width of the specimen, some correction of the reading should be introduced. From

elementary geometry applied to the problem shown in Fig. 5, where r is the radius of a specimen and d is the distance between the lens of a camera and the center of a specimen, the corrected radius can be derived as Eq. 1.

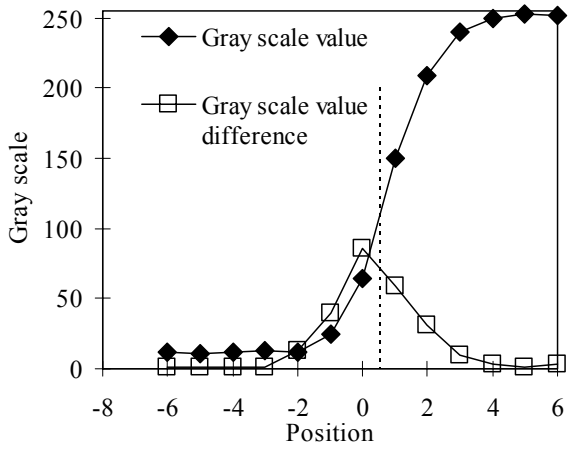

Fig. 4. Digitized edge of specimen

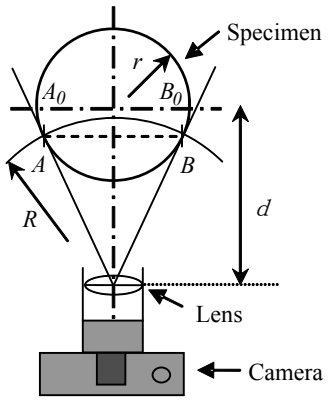

Fig. 5. Correction of measurement

$$r_{cor} = r\left(\cos\left(\arcsin\frac{r}{d}\right)-1\right), \quad (1)$$

where r_{cor} differs from r by about 1 % of their absolute value.

The basic tools of image processing can be found in any relevant book, e.g. [4]. However, in order to present a compact description of the presented method, all important steps of the method are explained in the following. The flowchart of the method, which was used for the image processing, is shown in Fig. 6.

Input: The functions used for conversion of the image were those for monochromatic 256 gray scale bitmaps, therefore the format of the input files needed to obey the format requirements. In order to minimize the effect of a local damage of a specimen, the input batch consisted of three images representing three stripes which were cut out of the overall image of a specimen.

Routine 1: The conversion of a bitmap into an array of digits can be achieved by a selection of a proper function available in a programming language. The commonly used programming languages provide such functions and the programming languages which are designed primarily for numerical calculations, such as the Fortran family, can import the graphics functions from other languages, such as C++. However, for those who seek the easiest way of converting a bitmap into digits without unnecessary delving into the world of computer graphics, the commercial product Matlab, or Mathematica, is recommended. These program packages offer an easy-to-use one-function conversion from a file to a file.

Routine 2: The file obtained from the conversion of a rectangular image is usually in the format: the number of pixels in a row or a column, the number of pixel in a column or a row, and the values of pixels written row by row or column by column. The edge detection requires some measures to be taken during capturing the image, such as spot lighting and a dark curtain behind the set in order to amplify the contrast on the gray scale. For the edge detection, it is necessary to exclude the effect of inhomogeneities imposed, e.g. by holes in the surface of a specimen caused by air bubbles. Such holes under an intensive illumination transpire as dark spots which, once only a very narrow strip had been cut out of the image, may delude the edge detecting routine. For this reason, it is desirable to allow a height of a strip to be at least twice the size of the largest inhomogeneity near an edge. The values in a column are then averaged so that the chance of erroneous edge detection is reduced.

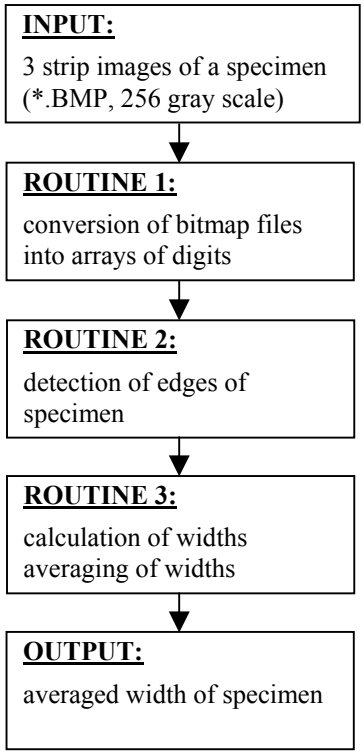

Fig. 6. Flow of image processing

After averaging the pixel values in each column a vector with the number of entries equal to the number of the columns is obtained. The values in the vector range from zero to 255 where zero means black and 255 means white color, the extreme values on the gray scale. Because the edge actually means the greatest difference between the color of a specimen and the color of a curtain on the

monochromatic gray scale, the vector of the absolute values of the pixels is converted to a vector of the differences between neighboring pixels. In this way the initial localization can be done, which is to find the position with the greatest value in the vector of the differences. The width of a specimen can be calculated by subtracting the number of pixels between the greatest values and converting it into the real width. However, this result obtained on the pixel domain is not always precise because the edge on an ordinary captured image is smeared over more than one pixel, as shown in Fig. 4. Then, it is necessary to shift the detection to the subpixel domain where this initial imprecision can be solved.

One of the possible methods how to acquire a more precise position of the actual edge is to find the center of the gravity of the area under the curve which connects the neighboring values near the initially localized edge. From the experience it is known that the edge of a light cylindrical plane contrasted against a dark background spreads over 5 to 10 pixels, while about 2000 pixels correspond with the diameter of a specimen. Then, because the shape of the curve connecting the neighboring values is not always an equilateral triangle, usually it inclines to a side, the center of gravity should be calculated for an area which is limited by the length of 3 to 7 pixels on both sides of the pixel with the greatest value.

An alternative method, which was described by Fu and Moosa in [5], suggests an approximation of the absolute values by a sixth-order polynomial in the vicinity of the greatest differences. The edge is then located at the inflexion point.

In this way, the edge is given no longer by an integer, which indexes the position of a pixel in the vector. The location of the edge is given as a real number defining a position inside a pixel.

Routine 3: The width of a specimen is calculated as the difference between the two real numbers indicating the position of the entries in the vector of the difference, which define the edges on both sides of a specimen. The conversion into a real width is conducted with respect to the mm/pixel ratio. However, for the investigation of the Poisson's ratio the conversion is not necessary since only the relative changes in the widths corresponding with various load levels are of interest.

In order to minimize the error of each edge detection, the three widths, which were calculated for each strip, are averaged.

Output: The output of the method consists of three widths calculated for the three respective strips, so that the change in the lateral deformation at three different places can be monitored, and the averaged width of a specimen.

4. RESULTS AND DISCUSSION

The accuracy of the proposed method was verified on a series of images captured on an unloaded specimen. The specimen was a standard cylinder of width of 100 mm. Also, the proposed edge detecting method (the center of gravity method) was compared with the method designed by Fu and Moosa, [5], for measurement of steel beam deflection. The accuracy and the comparison shown in Fig. 7 stand for a partial verification of the proposed method.

The proposed method was used for measuring the lateral deformation of standard cylindrical specimens subjected to uniaxial compressive loading. The images were obtained for two types of concrete, made of rapid hardening portland cement, which correspond to those used for investigation of the deformational behavior of concrete subjected to short-time and sustained loading at extremely early ages (described in [2]). The mix proportions of concrete are shown in Table 1, where 30 MPa and 60 MPa are the target 28 day compressive strengths.

Table 1. Mix proportions of two types of concrete

Type	Weight per unit volume (kg/m^3)			
	W	C	S	A
30 MPa	168	271	767	1136
60 MPa	181	490	599	1093

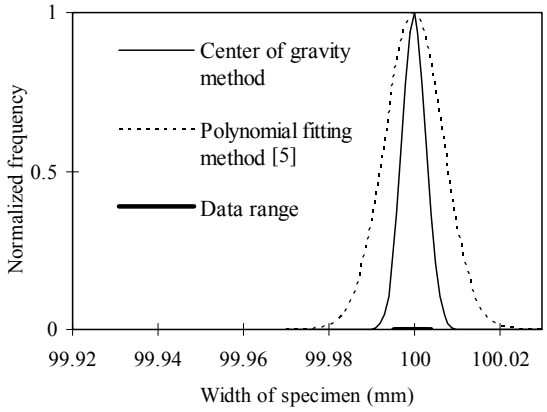

Fig. 7. Comparison between two methods

The apparent Poisson's ratio as a function of load level (f/f_c), where f stands for actual compressive stress and f_c stands for compressive strength at the moment of loading, is shown in Fig. 8. Due to inconsistent readings of both the longitudinal and lateral deformations related to settling of a specimen at the beginning of loading the readings of the apparent Poisson's ratio below the load level of about 20 % is excluded.

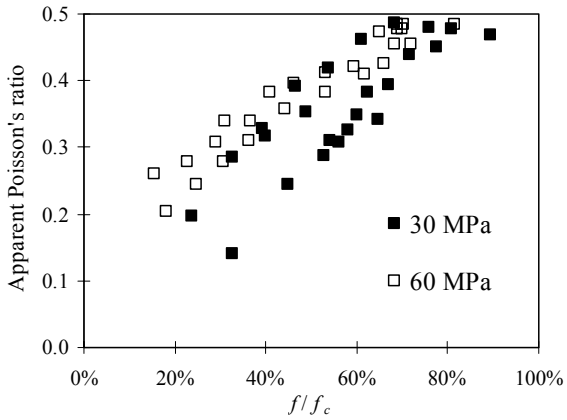

Fig. 8. Poisson's ratio of two types of concrete

The data in Fig. 8 were collected for ages of 4 to 6 hours and 3 to 5 hours for the concrete types 30 MPa and

60 MPa, respectively. Even though it was intended to show the effect of the rapidly progressing hydration in the data, no clear tendency of any evolution could be identified due to the scatter of the data readings. Nevertheless, the data in Fig. 8 clearly define a band of possible values of the apparent Poisson's ratio as a function of applied load level.

Fig. 8 further shows that the value 0.5 of the Poisson's ratio is reached at the load level of 80 %. This is explained by occurrence of vertical cracks transpiring along the whole height of a specimen by reaching the load level of 80 %, which were observed during the experiments.

For a multi-dimensional analysis, which in the case of concrete at the ages ranging from the initial time to the final setting time involves mainly compressive loading conditions, the Poisson's ratio, μ, can be expressed by a tri-linear function

$$\begin{aligned} \mu(S) &= 0.25 && S \in \langle 0;0.3 \rangle \\ \mu(S) &= 0.25 + 0.5(S - 0.3) \quad \textit{for} && S \in \langle 0.3;0.8 \rangle \\ \mu(S) &= 0.5 && S \in \langle 0.8;1 \rangle \end{aligned} ; \qquad (2)$$

$$S = \frac{f}{f_c} , \qquad (3)$$

where f is stress at the instant of loading and f_c is compressive strength at the instant of loading. f is known at the moment of loading and f_c can be readily obtained from the standard uniaxial compression test.

5. CONCLUSIONS

In this paper, a method for measuring lateral deformation of hardening concrete is presented. The method consists of capturing an image of a specimen subjected to loading in a simple standard uniaxial compression test by a high-resolution CCD camera and measurement of distances between the edges of the loaded specimen captured in the image with help of tools known from image analysis. This method only requires a standard loading system used for uniaxial compression test and a high-resolution CCD camera, which makes the method easy to apply and relatively inexpensive. Also, the accuracy of the method is very satisfactory. The test configuration is shown and the image processing method is described in detail.

A set of experimental data on the apparent Poisson's ratio for two types of concrete obtained at the ages ranging from 3 to 6 hours, along with an approximate relation between the Poisson's ratio and load level, are shown to demonstrate usefulness of the proposed method.

Acknowledgments

This work was supported by the Grant Agency of the Czech Republic (grant no. 103/05/2244), which is gratefully acknowledged.

REFERENCES

1. **Byfors, J.** Plain Concrete at Early Ages. Stockholm, Swedish Cement and Concrete Research Institute, 1980.
2. **Štemberk, P., Tsubaki, T.** 2003. Uniaxial Deformational Behavior and its Modeling of Solidifying Concrete under Short-time and Sustained Loading *Journal of Applied Mechanics JSCE* 6 2003: pp. 437 – 444.
3. GERMANN Instruments, Inc. 4C – Temperature & Stress; Temperature and Stress Simulation During Hardening – User Manual, GERMANN Instruments, Inc., Evanston, Illinois, 1998.
4. **Gonzalez, R., Woods, R.** Digital Image Processing. Prentice-Hall, Inc., New Jersey, 2002.
5. **Fu, G., Moosa, A.G.** An Optical Approach to Structural Displacement Measurement and Its Application *Journal of Engineering Mechanics ASCE* 128 (5) 2002: pp. 511 – 520.